Differences in composition of interdigital skin microbiota predict sheep and feet that develop footrot, a globally important cause of lameness in sheep

Rachel Clifton (r.clifton@bham.ac.uk)
University of Birmingham
Emma M Monaghan
University of Birmingham
Martin J Green
University of Nottingham
Kevin J Purdy
University of Warwick
Laura E Green
University of Birmingham

Research Article

Keywords: metagenomics, footrot, sheep, microbiota, 16S sequencing

Posted Date: October 19th, 2021

DOI: https://doi.org/10.21203/rs.3.rs-989108/v1

Version of Record: A version of this preprint was published at Scientific Reports on May 27th, 2022. See the published version at https://doi.org/10.1038/s41598-022-12772-7.

Abstract

Footrot has a major impact on health and productivity of sheep worldwide. The current paradigm for footrot pathogenesis is that physical damage to the interdigital skin (IDS) facilitates invasion of the essential pathogen *Dichelobacter nodosus*. The composition of the IDS microbiota is different in healthy and diseased feet, so an alternative hypothesis is that changes in the IDS microbiota facilitate footrot. We investigated the composition and diversity of the IDS microbiota of ten sheep, five that did develop footrot and five that did not (healthy) at weekly intervals for 20 weeks. The IDS microbiota was less diverse on sheep 2+ weeks before they developed footrot than on healthy sheep. This change could be explained by only seven of >2000 bacterial taxa detected. The incubation period of footrot is 8-10 days, and there was a further reduction in microbial diversity on feet that developed footrot in that incubation period. We conclude that there are two stages of dysbiosis in footrot: the first predisposes sheep to footrot and the second occurs in feet during the incubation of footrot. These findings change the paradigm of footrot pathogenesis.

Introduction

Ovine footrot is an infectious dermatitis of the interdigital skin (IDS) of sheep that causes lameness, reducing health and productivity in sheep worldwide (Marshall et al., 1991; Nieuwhof et al., 2008; Wassink et al., 2010b; Rather et al., 2011). In the UK, footrot is endemic (Prosser et al., 2019) with > 99% flocks affected (Monaghan et al., 2021) and an average within-flock prevalence of footrot of 3.5% (Prosser et al., 2020). Approximately 3 million sheep (20% of the breeding population) become lame each year (Winter et al., 2015) with economic losses of £24-£80 million per annum (Nieuwhof & Bishop, 2005; Wassink et al., 2010b).

Footrot is an inflammatory disease of the IDS. *Dichelobacter nodosus* is the essential pathogen (Beveridge, 1941; Kennan et al., 2011), and it increases in load before clinical signs occur (Witcomb et al., 2014). Once footrot has developed several bacteria increase in dominance including *Fusobacterium necrophorum* (Beveridge, 1941; Witcomb et al., 2014), Spirochaetes (Beveridge, 1941), and *Porphyromonas* (Maboni et al., 2017; McPherson et al., 2019). The microbial community of feet with footrot is different from healthy feet (Maboni et al., 2017; McPherson et al., 2019), this is true of many diseases e.g. irritable bowel disease, metabolic disorders and periodontitis (Jeffery et al., 2012; Abusleme et al., 2013; Le Chatelier et al., 2013), however, given the physiological and immunological changes in diseased individuals, alteration of the microbiome in diseased states is not surprising and does not infer a causal role for microbiomes in pathogenesis.

The gingival crevice is similar to IDS in that it is where ‘dead’ tooth and ‘dead’ horn abut living skin. Both sites are moist and have areas that are less oxygenated than others, and both have a microbiome. The current paradigm for the pathogenesis of periodontitis is that the keystone pathogen *Porphyromonas gingivalis* facilitates the development of a dysbiotic microbial community (Hajishengallis et al., 2011; Hajishengallis et al., 2012; Maekawa et al., 2014; Lamont et al., 2018), whilst the current paradigm for the

pathogenesis of footrot is that coarse grass or moisture damage the IDS, and that this physical damage is necessary for *D. nodosus* to invade the skin (Beveridge, 1941; Graham & Egerton, 1968; McPherson et al., 2021). Given the similarity between the IDS and the gingival crevice an alternative hypothesis for footrot is that dysbiosis of the IDS microbiota disrupts the integrity of the IDS through inflammation and facilitates invasion of *D. nodosus*.

As well as advancing scientific knowledge, understanding whether the IDS microbiota has a role in pathogenesis of footrot could provide new approaches to managements for control of footrot. In the UK, farmers currently control footrot using a combination of antimicrobial treatment of diseased sheep within three days of onset of footrot (Kaler et al., 2010; Wassink et al., 2010b), biosecurity and a mildly effective vaccine (Hindmarsh et al., 1989). Treatment of footrot accounts for 65% of antibiotic use on sheep farms (Davies et al., 2017) and controlling footrot requires constant management. Many farmers find the managements onerous (O'Kane et al., 2017) and would prefer a more simple, efficient alternative disease control tool (Wassink et al., 2010a).

The aim of our study was to investigate the IDS microbiota before and during footrot to elucidate whether there is a role of the microbiota in disease initiation.

Results

Selection of sheep and definition of diseased and healthy feet and sheep

We observed the 160 feet of 40 sheep from one lowland flock in Warwickshire, UK, weekly for 20 weeks. Footrot phenotype (Moore et al., 2005) and a swab sample from the IDS (Fig. 1a) were collected each week from each foot (Clifton et al., 2019). After the study was complete a subset of 10 sheep were selected for sequencing analysis (Fig. S1). This comprised five sheep with 20 healthy feet (H – healthy foot from healthy sheep) throughout the 20 week study and five sheep that developed footrot on 12 feet (D – diseased foot at some point in the 20 weeks of diseased sheep) with the other eight feet remaining healthy throughout the study (HD - healthy feet of diseased sheep) (Fig. 1c). Footrot was defined as inflammation of the IDS (interdigital dermatitis) score > 1 (Moore et al., 2005) and / or any separation of hoof horn from the living dermis (severe footrot) (Fig. 1a). There were 18 episodes of footrot in the 12 diseased feet that lasted 1 - 8 weeks (Fig. 1b).

The microbiota of the interdigital skin is temporally dynamic

There were 620 swab samples; 400 samples from sheep with footrot (D and HD feet) from each of the 20 weeks, and 220 samples from sheep that remained healthy (H) from weeks 1-3 and then 8 alternate weeks (Fig. 1c). After quality control, 16S rRNA gene sequencing data from 603 samples (218 - H, 229 - D and 156 - HD) were analysed. A total of 2,723 bacterial operational taxonomic units (OTUs) were

identified across all 603 samples. For 409 samples, additional data on bacterial load of *D. nodosus* estimated by qPCR (Witcomb et al., 2014) from a previous study were used (Clifton et al., 2019).

Initially we examined the level of similarity across all microbial communities of H, HD and D feet using four different distance measures: root Jensen Shannon distance (rJSD), Bray Curtis, and weighted and unweighted Unifrac. The IDS microbiota changed over time with all measures (Fig. 2 and S2) with communities that were temporally close more similar to each other than those that were temporally distant. Patterns were consistent across all feet irrespective of sheep or feet definition indicating an external influence, possibly the environment since changes correlated with change in soil moisture (Fig S3). There was no evidence of samples clustering by foot status or sheep (Fig. S4 and S5).

Composition of healthy sheep IDS microbiota is predictive of which sheep subsequently develop footrot

To determine whether composition of the IDS microbiota was predictive of which sheep subsequently developed footrot, we used a supervised machine learning approach. Samples from feet of sheep that developed footrot (D and HD) 2+ weeks before the first episode of disease occurred in that sheep were selected (week 1 for sheep 3535, weeks 1-2 for sheep 3514 and weeks 1-4 for sheep 3478, 3488 and 3547). Samples from H feet from the same time period were also included (weeks 1-3; Fig. 1c) providing a total of 117 samples (60 - H, 32 - D and 25 - HD) for classification. Because time was linked to OTUs (Fig. 2), a random forest model was used to identify OTUs that were strongly correlated with time in H feet and those OTUs were removed from the dataset prior to analysis. We implemented random forest and stochastic gradient boosting algorithms with recursive feature elimination to identify OTUs that classified H feet as belonging to healthy sheep and HD and D feet as belonging to diseased sheep. To increase robustness (Lima et al., 2020), only OTUs identified by both algorithms were considered important.

Sheep that developed footrot were differentiated from those that did not with a mean cross-validation accuracy of 0.71 for the random forest algorithm and 0.69 for the stochastic gradient boosting algorithm. Seven of the 2,723 OTUs were identified by both algorithms (Fig. 3a and b); all seven were more present and abundant on D and HD than H feet (Table 1 and Fig. 3c). The Inverse Simpson index was significantly higher in H feet than HD and D feet (Fig. 4 and Table S1), indicating that even during periods of health, the IDS communities from sheep that developed footrot were different from those that remained healthy.

Within the seven differentiating OTUs, there were two members of the genus *Porphyromonas* and one from the genus *Prevotella* (Fig. 3c) both associated with disease in humans and sheep (Kamma et al., 1994; Hajishengallis et al., 2011; Borsanelli et al., 2017; Maboni et al., 2017; McPherson et al., 2019), OTU_23 was a member of the genus *Pseudoclavibacter*, with occasional pathogenicity (Lemaitre et al., 2011; Oyaert et al., 2013; Pailhoriès et al., 2014), and we were unable to determine an accurate taxonomic identification for OTU_190, OTU_69 and OTU_364 using the Genbank database (Fig. S6).

Table 1
Frequency of detection of eight OTUs used to predict disease status on D, HD and H feet in the period 2+ weeks before footrot occurred.

		Percentage of samples with OTU detected		
	Taxonomic identification	D feet (n=32)	HD feet (n=25)	H feet (n=60)
OTU_41	*Prevotella*	84	92	77
OTU_190	(Tissierellales)	84	96	40
OTU_69	(Bacteroidia)	53	56	0
OTU_28	*Porphyromonas*	94	96	58
OTU_23	*Pseudoclavibacter*	72	76	35
OTU_61	*Porphyromonas*	50	60	3
OTU_364	(Tissierellales)	59	56	7

Diversity of the interdigital skin microbiota decreases prior to footrot

Linear mixed effects models of Inverse Simpson Index showed that there was a reduction in OTU diversity on D feet one week before the onset of footrot, which resolved one week after footrot resolved (Fig. 4 and Table S2). OTU diversity on D feet 2+ weeks before the onset of footrot did not differ from diversity on HD feet.

Discussion

Our study provides the first evidence that the IDS microbiota has a causal role in the pathogenesis of footrot. Dysbiosis occurs in two phases, initially sheep become predisposed to footrot, and then, after predisposed feet are infected with *D. nodosus*, the microbiota changes again in the incubation period and then feet become diseased. We discuss the IDS microbiota in healthy and predisposed sheep, and feet incubating footrot and propose new hypotheses for the pathogenesis of footrot.

Sheep that developed footrot had a different IDS microbiota from sheep that remained healthy from the start of the study and before the incubation period for footrot; we hypothesise that this predisposed them to disease. It was not possible to determine whether this difference in community composition is permanent or temporary, only that it was present from the start of the study. The predisposed dysbiotic microbiota was less diverse than the healthy microbiota (Fig. 4), and varied from the healthy microbiota with the presence and abundance of seven OTUs out of over 2000 (Table 1 and Fig. 3c). This is a very small number of OTUs and with the model fitting approach used (Lima et al., 2020), which minimises detection of false positive associations, it is highly likely these are true differences in the microbiota.

Among the seven OTUs were *Porphyromonas* and *Prevotella* species. *Prevotella* and *Porphyromonas* are present in IDS of feet with footrot (Maboni et al., 2017; McPherson et al., 2019) but their role in disease initiation was unknown until this report. Both *Porphyromonas* and *Prevotella* subvert the host immune system (Hajishengallis et al., 2011; Maekawa et al., 2014; Ilhan et al., 2020; Iljazovic et al., 2021), and we hypothesise that they facilitate dysbiosis and a pro-inflammatory state which damages the integrity of the IDS and enables *D. nodosus* to invade the epidermis. This predisposing dysbiosis was present two or more weeks before footrot developed, longer than the 8-10 day incubation period of footrot (Egerton et al., 1969; Roberts & Egerton, 1969) indicating that it is causal, initiating footrot, rather than on the causal pathway. Bacterial inflammation in the epidermis is an alternative explanation to the current paradigm that physical damage of the IDS is necessary for footrot to occur (Beveridge, 1941; Graham & Egerton, 1968).

In sheep predicted to develop footrot there was a further reduction in bacterial diversity in D feet one week before clinical signs developed (Fig. 4). This is the incubation period when the load of *D. nodosus* increases (Witcomb et al., 2014), it lasts 8-10 days (Egerton et al., 1969; Roberts & Egerton, 1969). Typically, only one foot of a sheep becomes diseased (personal observation). This is probably because *D. nodosus* contaminates pasture in heterogenous 'foot prints' from infectious feet with high concentrations of *D. nodosus* (Witcomb et al., 2014), and only at certain sites (Clifton et al., 2019), and so only some feet are contaminated with *D. nodosus* as sheep graze.

The IDS microbiota was temporally dynamic, with communities more similar in time across sheep than over time within sheep (Fig. 2). By accounting for confounding effects of the change in the IDS microbiota over time on diversity and community composition, we were able to identify relationships between the microbiota and disease. We hypothesise that change in environmental conditions over time led to a change in OTUs on the IDS; throughout the twenty week study the soil moisture changed from wet to dry and the temperature gradually increased (Clifton et al., 2019). It is possible that these environmental changes facilitate dysbiosis by favouring colonisation with *Porphyromonas* and *Prevotella* spp; this would agree with existing knowledge that footrot is closely linked to the environmental conditions, in particular soil moisture (Graham & Egerton, 1968; Kaler et al., 2012; Sreenivasulu et al., 2013; Smith et al., 2014; Clifton et al., 2019).

The current approach to management of footrot is to treat diseased sheep, our results suggest that managing the IDS microbiota could provide an alternative approach. This could be management interventions that favour development of a protective microbiota, or through the use of novel microbiome-based therapeutics; such approaches are being increasingly adopted in human medicine (Wong & Levy, 2019). Clearly considerable work is required to develop these ideas but the novel findings in the current paper provide a new avenue to consider alternative approaches to present treatments.

In conclusion, there are two stages of dysbiosis of the interdigital skin: the first predisposes sheep to colonisation with *D. nodosus* and so initiates footrot, with remarkably only seven OTUs predicting susceptible sheep. The second arises in feet during incubation through to disease. These highly novel

results revolutionise our understanding of the role of bacteria in the pathogenesis of footrot in sheep, an understanding that had not changed since 1941 (Beveridge, 1941).

Methods

Study sample and data collection

Collection of samples and metadata for this study are described in Clifton et al. (2019) and ethical approval for this original study was obtained from the University or Warwick's local ethical committee; the Animal Welfare & Ethical Review Body (AWERB.33/13-14). Briefly, the data collection ran for 20 weeks from February to July 2015. In week 1 a group of 120 ten-month old Suffolk X Wiltshire Horn sheep from one flock were examined for footrot phenotype by scoring lesions of interdigital dermatitis (ID) and severe footrot (SFR) on a scale of 0 to 4 where 0 indicates no lesion and increasing scores indicate increasing severity (Moore et al., 2005). Forty healthy sheep defined as ID score ≤ 1, SFR score = 0, were selected as the study sample. The interdigital skin (IDS) of each foot of the 40 sheep was swab sampled and then the sheep were immediately moved to a pasture that had not been stocked with any livestock for ≥ 10 days to ensure that it was free from *D. nodosus* (Beveridge, 1941). IDS swab samples and footrot phenotype scores were collected from the 40 sheep each week from weeks 2 to 20. In addition, data on daily rainfall and temperature, and weekly soil moisture and temperature were collected (Clifton et al., 2019).

Selection of a subset of sheep for sequencing analysis

Ten sheep, five that remained healthy and five that developed footrot at least once were selected for the current study based on observed foot scores (Fig. S1).There were 28/40 sheep that had at least one case of footrot; of these five were selected to provide a range of severities and durations of disease. Healthy sheep were defined as those with no occurrences of footrot; of these, the five with the highest number of occurrences of ID score = 0 were selected.

Library preparation for 16S rRNA gene sequencing

DNA was extracted from IDS swabs using the method described by Purdy (2005). The V1-V3 variable region of the bacterial 16S rRNA gene was amplified in a first stage PCR using the 27-YMF and 534R primers (Muyzer et al., 1993; Satokari et al., 2001) with overhanging adaptors for Illumina MiSeq sample preparation (Table S3). The 27-YMF and 534R primers were adapted to correct for mismatches with the *D. nodosus* 16S sequence (Calvo-Bado et al., 2011) (Table S3) and successful amplification of the *D. nodosus* VCS1703A strain 16S rRNA gene was confirmed prior to library preparation. Amplicons were purified using Agencourt AMPure XP magnetic beads (Beckman-Coulter, Brea, CA), normalised using the SequelPrep Normalisation Plate kit (Applied Biosystems, Warrington, UK), and pooled into two libraries for sequencing using 300bp paired-end Illumina MiSeq sequencing at the University of Warwick Genomics Facility.

Sampling, extraction and PCR controls.

An extraction control of sterile molecular biology grade water was used in all sets of DNA extractions and carried through to sequencing. All PCR plates also included DNA from a model community as a positive control (*Staphylococcus aureus*, *Escherichia coli*, *Streptococcus agalactiae*, *Streptococcus dysgalactiae* and *Streptococcus uberis*) and a PCR negative control of sterile molecular biology grade water. All controls were sequenced alongside the samples.

Processing of 16S rRNA gene sequencing data

Sequence data were processed using USEARCH version 8.1 (Edgar, 2010; Edgar & Flyvbjerg, 2015). All samples had reverse reads truncated by 30bp due to quality issues with the sequencing kits at the time. Forward and truncated reverse reads were then merged, allowing for ≤ 2 mismatches. Samples were quality filtered using a maximum error rate of 0.5% and minimum sequence length of 467bp. Data from the negative control samples were used to remove contaminant sequences (data filtered at 96% match), and the resulting filtered sequences were clustered into OTUs in USEARCH v8.1 at 97% similarity. An initial taxonomy was then assigned to each OTU in QIIME (Caporaso et al., 2010) using the Greengenes database (DeSantis et al., 2006). For OTUs identified in the data analysis as predicting disease status, taxonomic assignment was confirmed using nucleotide BLAST against the rRNA Bacteria and Archaea database with uncultured sequences excluded.

Statistical analysis of microbial communities

All analyses were conducted in the R statistical environment version 4.0.2 (R Core Team, 2020).

Determination of beta diversity distance measures

Data were converted to relative abundance (McMurdie & Holmes, 2014; McKnight et al., 2019) and pairwise dissimilarity between communities was calculated using four distance metrics (Root Jensen Shannon Distance (rJSD), Bray Curtis, and unweighted and weighted Unifrac) with the Phyloseq package in R (McMurdie & Holmes, 2013). Similarity between communities was visualised using principal coordinate analysis (PCoA).

Methods for determination of clustering based on beta diversity distance measures followed the principles described by Koren et al. (2013) and were adapted from the robust clustering algorithm developed by García-Jiménez and Wilkinson (2019). Clustering was performed using two approaches: the Partition Around Medoids (PAM) algorithm and hierarchical clustering. For each approach results were compared for the four distance metrics described above. Two types of clustering score (average Silhouette width (SI) and Prediction Strength (PS)) followed by an additional bootstrapping process (evaluated with the Jaccard similarity score) were used to determine whether there were distinct microbiome states (thresholds as described by Koren et al. (2013)), and to identify the optimum number of clusters (Fig. S7).

Use of machine learning to identify OTUs predictive of subsequent disease status

All models were implemented using the caret package (Kuhn, 2020). Prior to implementation of each model, unsupervised filtering was used to remove rare OTUs (those with fewer than 10 reads or present in fewer than 5% of samples). All predictors were standardised (mean subtracted and then divided by standard deviation) and those with near-zero variance (< 10% distinct values out of number of total samples and ratio of the frequency of the most common value to the frequency of the second most common value > 95/5) were removed.

A random forest regression with week of study as a continuous outcome was used to identify and remove 140 OTUs highly correlated with time. Only data from healthy sheep were included in this analysis (218 observations) and after filtering OTU data as described above, 2,319 OTUs were offered to the model. The model was fit to the data and hyperparameters optimised using leave-one-out cross-validation (data from one sheep left out each time). Visual assessment of the variable importance plot for the model was used to identify the OTUs to be removed (Fig. S8).

Two machine learning algorithms were used for classification of disease status: random forest (RF) and stochastic gradient boosting (GBM). The outcome variable of interest was whether a sheep later developed footrot or never developed footrot. After filtering out rare OTUs and those with near zero variance, there were 2,184 OTUs offered to each algorithm. A common approach to implementation of each algorithm was used as follows. First, each model was fit to the data and hyperparameters optimised using cross-validation with 25 folds created by leaving out each possible combination of one healthy and one diseased sheep (Fig. 5). For each algorithm, recursive feature elimination (RFE) (Kuhn & Johnson, 2019) was used to identify the smallest subset of features that was required for classification without compromising accuracy (Fig. S9). Subset sizes tested were 10, 20, 30, 40, 50, 100, 500, 1,000, 1,500, 2,000 and 2,184 features. An accuracy value that was within 5% of the maximum value was tolerated. The *N* most important features where *N* was the optimum subset size were identified for each algorithm based on feature rankings across all resampling iterations, and a reduced dataset was then created containing only those OTUs identified by both RF and GBM algorithms. This comprised seven OTUs. Classification was repeated with both algorithms using only seven OTUs to confirm that using the reduced dataset did not decrease model performance.

Repeating machine learning analyses with load of Dichelobacter nodosus included

There were 20 samples with high loads of *D. nodosus* (between 10^5 and 10^7 *rpoD* gene copies μl^{-1}) where the *D. nodosus* OTU was not detected within our data (Fig. S10). We confirmed that sequences belonging to *D. nodosus* were not wrongly assigned or filtered out during quality control, and so we conclude that there were mismatch issues with the V1-V3 primers. Given our primers successfully amplified the VCS1703A strain, we propose that strain level variability may occur at this region meaning that some strains are amplified more than others.

To test whether failure to detect the *D. nodosus* OTU impacted on model accuracy for predicting disease status, we repeated the machine learning analysis described above with bacterial load of *D. nodosus* included as an additional predictor variable. For the 194 samples where qPCR data was not available, load of *D. nodosus* was imputed using the Expectation-Maximisation with Bootstrapping algorithm (Honaker & King, 2010) in the Amelia II package (Honaker et al., 2011). Our results confirmed that inclusion of bacterial load of *D. nodosus* did not change model performance.

Determination of changes in alpha diversity with disease status

The Inverse Simpson index was estimated for all samples using the function provided within the Phyloseq package (McMurdie & Holmes, 2013). A linear mixed-effects model implemented in the lme4 package (Bates et al., 2015) was used to investigate associations between the Inverse Simpson index and disease status of feet. Inverse Simpson Index was right skewed and was therefore square root transformed prior to analysis (Fig. S11). A categorical variable for disease status was tested as a fixed effect with the following seven categories: H feet, HD feet, D feet 2+ weeks before onset of footrot, D feet 1 week before onset of footrot, D feet during a footrot episode, D feet 1 week after a footrot episode ended, and D feet 2+ weeks after a footrot episode ended. Sheep was included as a random effect to account for clustering of feet within sheep and a third order polynomial term for day of study was included as a fixed effect to account for underlying changes in diversity over time. Fitted versus residuals plots were visually assessed to check for non-linearity, unequal variances and outliers (Fig. S12), and posterior predictive simulation (Gelman & Hill, 2006; Bates et al., 2015) was used to check model fit.

Declarations

ACKNOWLEDGEMENTS

This study was funded by the Animal Research Club grant (BB/M012980/1) from the BBSRC, UK. Thanks to the farmer who allowed us to sample his sheep, and to Katharina Giebel, Jess Taylor and Zoë Willis for collecting samples and Katharina Giebel, Jess Taylor and Nicola Liu for assisting with laboratory analyses.

AUTHOR CONTRIBUTIONS

LEG and KJP conceptualised and designed the study. EM prepared samples for sequencing and processed sequence data. RC conducted statistical analyses with support from MJG and LEG. RC, LEG and MJG wrote the manuscript.

COMPETING INTERESTS

The authors declare no competing interests.

References

Abusleme, L., Dupuy, A. K., Dutzan, N., Silva, N., Burleson, J. A., Strausbaugh, L. D., Gamonal, J. & Diaz, P. I. (2013) The subgingival microbiome in health and periodontitis and its relationship with community biomass and inflammation. *Isme Journal*, 7 (5): 1016–1025.

Bates, D., Mächler, M., Bolker, B. & Walker, S. (2015) Fitting linear mixed-effects models using lme4. *Journal of Statistical Software*, 67 (1): 1–48.

Beveridge, W. I. B. (1941) Foot-rot in sheep: a transmissible disease due to infection with *Fusiformis nodosus* (n.sp.): studies on its cause, epidemiology and control. *CSIRO Australian Bulletin*, 140 1–56.

Borsanelli, A. C., Gaetti-Jardim, E., Jr., Schweitzer, C. M., Viora, L., Busin, V., Riggio, M. P. & Dutra, I. S. (2017) Black-pigmented anaerobic bacteria associated with ovine periodontitis. *Vet Microbiol*, 203 271–274.

Calvo-Bado, L. A., Oakley, B. B., Dowd, S. E., Green, L. E., Medley, G. F., Ul-Hassan, A., Bateman, V., Gaze, W., Witcomb, L., Grogono-Thomas, R., Kaler, J., Russell, C. L. & Wellington, E. M. H. (2011) Ovine pedomics: the first study of the ovine foot 16S rRNA-based microbiome. *The ISME Journal*, 5 (9): 1426–1437.

Caporaso, J. G., Kuczynski, J., Stombaugh, J., Bittinger, K., Bushman, F. D., Costello, E. K., Fierer, N., Peña, A. G., Goodrich, J. K., Gordon, J. I., Huttley, G. A., Kelley, S. T., Knights, D., Koenig, J. E., Ley, R. E., Lozupone, C. A., McDonald, D., Muegge, B. D., Pirrung, M., Reeder, J., Sevinsky, J. R., Turnbaugh, P. J., Walters, W. A., Widmann, J., Yatsunenko, T., Zaneveld, J. & Knight, R. (2010) QIIME allows analysis of high-throughput community sequencing data. *Nature Methods*, 7 (5): 335–336.

Clifton, R., Giebel, K., Liu, N. L. B. H., Purdy, K. J. & Green, L. E. (2019) Sites of persistence of Fusobacterium necrophorum and Dichelobacter nodosus: a paradigm shift in understanding the epidemiology of footrot in sheep. *Scientific Reports*, 9 (1): 14429.

Davies, P., Remnant, J. G., Green, M. J., Gascoigne, E., Gibbon, N., Hyde, R., Porteous, J. R., Schubert, K., Lovatt, F. & Corbishley, A. (2017) Quantitative analysis of antibiotic usage in British sheep flocks. *Veterinary Record*, 181 (19): 511.

DeSantis, T. Z., Hugenholtz, P., Larsen, N., Rojas, M., Brodie, E. L., Keller, K., Huber, T., Dalevi, D., Hu, P. & Andersen, G. L. (2006) Greengenes, a Chimera-Checked 16S rRNA Gene Database and Workbench Compatible with ARB. *Applied and Environmental Microbiology*, 72 (7): 5069.

Edgar, R. C. (2010) Search and clustering orders of magnitude faster than BLAST. *Bioinformatics*, 26 (19): 2460–2461.

Edgar, R. C. & Flyvbjerg, H. (2015) Error filtering, pair assembly and error correction for next-generation sequencing reads. *Bioinformatics*, 31 (21): 3476–3482.

Egerton, J. R., Roberts, D. S. & Parsonson, I. M. (1969) The aetiology and pathogenesis of ovine foot-rot. I. A histological study of the bacterial invasion. *Journal of Comparative Pathology*, 79 (2): 207–215.

García-Jiménez, B. & Wilkinson, M. D. (2019) Robust and automatic definition of microbiome states. *PeerJ*, 7 e6657.

Gelman, A. & Hill, J. (2006) *Data analysis using regression and multilevel/hierarchical models*. Cambridge university press.

Graham, N. P. & Egerton, J. R. (1968) Pathogenesis of ovine foot-rot: the role of some environmental factors. *Australian Veterinary Journal*, 44 (5): 235–240.

Hajishengallis, G., Darveau, R. P. & Curtis, M. A. (2012) The keystone pathogen hypothesis. *Nature reviews. Microbiology*, 10 (10): 717–725.

Hajishengallis, G., Liang, S., Payne, M. A., Hashim, A., Jotwani, R., Eskan, M. A., McIntosh, M. L., Alsam, A., Kirkwood, K. L., Lambris, J. D., Darveau, R. P. & Curtis, M. A. (2011) Low-abundance biofilm species orchestrates inflammatory periodontal disease through the commensal microbiota and complement. *Cell Host Microbe*, 10 (5): 497–506.

Hindmarsh, F., Fraser, J. & Scott, K. (1989) Efficacy of a multivalent *Bacteroides nodosus* vaccine against foot rot in sheep in Britain. *Veterinary Record*, 125 (6): 128–130.

Honaker, J. & King, G. (2010) What to do About Missing Values in Time Series Cross-Section Data. *American Journal of Political Science*, 54 (3): 561–581.

Honaker, J., King, G. & Blackwell, M. (2011) Amelia II: A Program for Missing Data. *Journal of Statistical Software*, 45 (7): 1–47.

Ilhan, Z. E., Łaniewski, P., Tonachio, A. & Herbst-Kralovetz, M. M. (2020) Members of Prevotella Genus Distinctively Modulate Innate Immune and Barrier Functions in a Human Three-Dimensional Endometrial Epithelial Cell Model. *The Journal of Infectious Diseases*, 222 (12): 2082–2092.

Iljazovic, A., Roy, U., Gálvez, E. J. C., Lesker, T. R., Zhao, B., Gronow, A., Amend, L., Will, S. E., Hofmann, J. D., Pils, M. C., Schmidt-Hohagen, K., Neumann-Schaal, M. & Strowig, T. (2021) Perturbation of the gut microbiome by Prevotella spp. enhances host susceptibility to mucosal inflammation. *Mucosal Immunology*, 14 (1): 113–124.

Jeffery, I. B., O'Toole, P. W., Öhman, L., Claesson, M. J., Deane, J., Quigley, E. M. & Simrén, M. (2012) An irritable bowel syndrome subtype defined by species-specific alterations in faecal microbiota. *Gut*, 61 (7): 997–1006.

Kaler, J., Daniels, S. L. S., Wright, J. L. & Green, L. E. (2010) Randomized clinical trial of long-acting oxytetracycline, foot trimming, and flunixine meglumine on time to recovery in sheep with footrot. *Journal*

of Veterinary Internal Medicine, 24 (2): 420–425.

Kaler, J., Wani, S. A., Hussain, I., Beg, S. A., Makhdoomi, M., Kabli, Z. A. & Green, L. E. (2012) A clinical trial comparing parenteral oxytetracyline and enrofloxacin on time to recovery in sheep lame with acute or chronic footrot in Kashmir, India. *BMC Veterinary Research*, 8

Kamma, J. J., Nakou, M. & Manti, F. A. (1994) Microbiota of rapidly progressive periodontitis lesions in association with clinical parameters. *J Periodontol*, 65 (11): 1073–1078.

Kennan, R. M., Han, X. Y., Porter, C. J. & Rood, J. I. (2011) The pathogenesis of ovine footrot. *Veterinary Microbiology*, 153 (1-2): 59–66.

Koren, O., Knights, D., Gonzalez, A., Waldron, L., Segata, N., Knight, R., Huttenhower, C. & Ley, R. E. (2013) A Guide to Enterotypes across the Human Body: Meta-Analysis of Microbial Community Structures in Human Microbiome Datasets. *PLOS Computational Biology*, 9 (1): e1002863.

Kuhn, M. (2020) caret: Classification and Regression Training. https://CRAN.R-project.org/package=caret.

Kuhn, M. & Johnson, K. (2019) *Feature engineering and selection: A practical approach for predictive models*. CRC Press.

Lamont, R. J., Koo, H. & Hajishengallis, G. (2018) The oral microbiota: dynamic communities and host interactions. *Nature reviews. Microbiology*, 16 (12): 745–759.

Le Chatelier, E., Nielsen, T., Qin, J., Prifti, E., Hildebrand, F., Falony, G., Almeida, M., Arumugam, M., Batto, J. M., Kennedy, S., Leonard, P., Li, J., Burgdorf, K., Grarup, N., Jørgensen, T., Brandslund, I., Nielsen, H. B., Juncker, A. S., Bertalan, M., Levenez, F., Pons, N., Rasmussen, S., Sunagawa, S., Tap, J., Tims, S., Zoetendal, E. G., Brunak, S., Clément, K., Doré, J., Kleerebezem, M., Kristiansen, K., Renault, P., Sicheritz-Ponten, T., de Vos, W. M., Zucker, J. D., Raes, J., Hansen, T., Bork, P., Wang, J., Ehrlich, S. D. & Pedersen, O. (2013) Richness of human gut microbiome correlates with metabolic markers. *Nature*, 500 (7464): 541–546.

Lemaitre, F., Stein, A., Raoult, D. & Drancourt, M. (2011) Pseudoclavibacter-like subcutaneous infection: a case report. *Journal of Medical Case Reports*, 5 (1): 468.

Lima, E., Davies, P., Kaler, J., Lovatt, F. & Green, M. (2020) Variable selection for inferential models with relatively high-dimensional data: Between method heterogeneity and covariate stability as adjuncts to robust selection. *Scientific Reports*, 10 (1): 8002.

Maboni, G., Blanchard, A., Frosth, S., Stewart, C., Emes, R. & Tötemeyer, S. (2017) A distinct bacterial dysbiosis associated skin inflammation in ovine footrot. *Scientific Reports*, 7 45220.

Maekawa, T., Krauss, J. L., Abe, T., Jotwani, R., Triantafilou, M., Triantafilou, K., Hashim, A., Hoch, S., Curtis, M. A., Nussbaum, G., Lambris, J. D. & Hajishengallis, G. (2014) Porphyromonas gingivalis manipulates

complement and TLR signaling to uncouple bacterial clearance from inflammation and promote dysbiosis. *Cell Host Microbe*, 15 (6): 768–778.

Marshall, D. J., Walker, R. I., Cullis, B. R. & Luff, M. F. (1991) The effect of footrot on body weight and wool growth of sheep. *Australian Veterinary Journal*, 68 (2): 45–49.

McKnight, D. T., Huerlimann, R., Bower, D. S., Schwarzkopf, L., Alford, R. A. & Zenger, K. R. (2019) Methods for normalizing microbiome data: An ecological perspective. *Methods in Ecology and Evolution*, 10 (3): 389–400.

McMurdie, P. J. & Holmes, S. (2013) phyloseq: An R Package for Reproducible Interactive Analysis and Graphics of Microbiome Census Data. *PLOS ONE*, 8 (4): e61217.

McMurdie, P. J. & Holmes, S. (2014) Waste Not, Want Not: Why Rarefying Microbiome Data Is Inadmissible. *PLOS Computational Biology*, 10 (4): e1003531.

McPherson, A. S., Dhungyel, O. P. & Whittington, R. J. (2019) The microbiome of the footrot lesion in Merino sheep is characterized by a persistent bacterial dysbiosis. *Veterinary Microbiology*, 236 108378.

McPherson, A. S., Whittington, R. J., Kennan, R. M., Rood, J. I. & Dhungyel, O. P. (2021) A pasture-based experimental infection model for footrot in sheep. *Small Ruminant Research*, 195 106305.

Monaghan, E. M., Prosser, N. S., Witt, J., Lewis, K. E., Nabb, E., Keeling, M. J., Purdy, K. J. & Green, L. E. (2021) Impact of Strain Variation of Dichelobacter nodosus on Disease Severity and Presence in Sheep Flocks in England. *Frontiers in veterinary science*, 8 713927–713927.

Moore, L. J., Wassink, G. J., Green, L. E. & Grogono-Thomas, R. (2005) The detection and characterisation of Dichelobacter nodosus from cases of ovine footrot in England and Wales. *Vet Microbiol*, 108 (1-2): 57–67.

Muyzer, G., De Waal, E. C. & Uitterlinden, A. G. (1993) Profiling of complex microbial populations by denaturing gradient gel electrophoresis analysis of polymerase chain reaction-amplified genes coding for 16S rRNA. *Applied and environmental microbiology*, 59 (3): 695–700.

Nieuwhof, G. J. & Bishop, S. C. (2005) Costs of the major endemic diseases of sheep in Great Britain and the potential benefits of reduction in disease impact. *Animal Science*, 81 23–29.

Nieuwhof, G. J., Bishop, S. C., Hill, W. G. & Raadsma, H. W. (2008) The effect of footrot on weight gain in sheep. *Animal*, 2 (10): 1427–1436.

O'Kane, H., Ferguson, E., Kaler, J. & Green, L. (2017) Associations between sheep farmer attitudes, beliefs, emotions and personality, and their barriers to uptake of best practice: The example of footrot. *Preventive Veterinary Medicine*, 139 (Pt B): 123–133.

Oyaert, M., De Baere, T., Breyne, J., De Laere, E., Mariën, S., Waets, P. & Laffut, W. (2013) First Case of Pseudoclavibacter bifida Bacteremia in an Immunocompromised Host with Chronic Obstructive Pulmonary Disease (COPD). *Journal of Clinical Microbiology*, 51 (6): 1973–1976.

Pailhoriès, H., Lemarié, C., Quinqueneau, C., Eveillard, M., Baufreton, C., Rouleau, F., Mahaza, C., Joly-Guillou, M.-L. & Kempf, M. (2014) First report of endocarditis caused by a Pseudoclavibacter species. *Journal of clinical microbiology*, 52 (9): 3465–3467.

Prosser, N. S., Monaghan, E. M., Green, L. E. & Purdy, K. J. (2020) Serogroups of Dichelobacter nodosus, the cause of footrot in sheep, are randomly distributed across England. *Scientific Reports*, 10 (1): 16823.

Prosser, N. S., Purdy, K. J. & Green, L. E. (2019) Increase in the flock prevalence of lameness in ewes is associated with a reduction in farmers using evidence-based management of prompt treatment: A longitudinal observational study of 154 English sheep flocks 2013–2015. *Preventive Veterinary Medicine*, 173 104801.

Purdy, K. J. (2005) Nucleic acid recovery from complex environmental samples. *Methods in Enzymology*, 397: 271–292.

R Core Team (2020) R: A language and environment for statistical computing. http://www.R-project.org.

Rather, M. A., Wani, S. A., Hussain, I., Bhat, M. A., Kabli, Z. A. & Magray, S. N. (2011) Determination of prevalence and economic impact of ovine footrot in central Kashmir India with isolation and molecular characterization of *Dichelobacter nodosus*. *Anaerobe*, 17 (2): 73–77.

Roberts, D. S. & Egerton, J. R. (1969) The aetiology and pathogenesis of ovine foot-rot. II. The pathogenic association of *Fusiformis nodosus* and *Fusiformis necrophorus*. *Journal of Comparative Pathology*, 79 (2): 217–227.

Satokari, R. M., Vaughan, E. E., Akkermans, A. D., Saarela, M. & de Vos, W. M. (2001) Bifidobacterial diversity in human feces detected by genus-specific PCR and denaturing gradient gel electrophoresis. *Appl Environ Microbiol*, 67 (2): 504–513.

Smith, E. M., Green, O. D. J., Calvo-Bado, L. A., Witcomb, L. A., Grogono-Thomas, R., Russell, C. L., Brown, J. C., Medley, G. F., KilBride, A. L., Wellington, E. M. H. & Green, L. E. (2014) Dynamics and impact of footrot and climate on hoof horn length in 50 ewes from one farm over a period of 10 months. *Veterinary Journal*, 201 (3): 295–301.

Sreenivasulu, D., Vijayalakshmi, S., Raniprameela, D., Karthik, A., Wani, S. A. & Hussain, I. (2013) Prevalence of ovine footrot in the tropical climate of southern India and isolation and characterisation of *Dichelobacter nodosus*. *Revue Scientifique et Technique - Office International des Épizooties*, 32 (3): 869–877.

Wassink, G. J., George, T. R. N., Kaler, J. & Green, L. E. (2010a) Footrot and interdigital dermatitis in sheep: Farmer satisfaction with current management, their ideal management and sources used to adopt new strategies. *Preventive Veterinary Medicine*, 96 (1): 65–73.

Wassink, G. J., King, E. M., Grogono-Thomas, R., Brown, J. C., Moore, L. J. & Green, L. E. (2010b) A within farm clinical trial to compare two treatments (parenteral antibacterials and hoof trimming) for sheep lame with footrot. *Preventive Veterinary Medicine*, 96 (1-2): 93–103.

Winter, J. R., Kaler, J., Ferguson, E., KilBride, A. L. & Green, L. E. (2015) Changes in prevalence of, and risk factors for, lameness in random samples of English sheep flocks: 2004-2013. *Preventive Veterinary Medicine*, 122 (1-2): 121–128.

Witcomb, L. A., Green, L. E., Kaler, J., Ul-Hassan, A., Calvo-Bado, L. A., Medley, G. F., Grogono-Thomas, R. & Wellington, E. M. H. (2014) A longitudinal study of the role of *Dichelobacter nodosus* and *Fusobacterium necrophorum* load in initiation and severity of footrot in sheep. *Preventive Veterinary Medicine*, 115 (1-2): 48–55.

Wong, A. C. & Levy, M. (2019) New approaches to microbiome-based therapies. *MSystems*, 4 (3): e00122-00119.

Figures

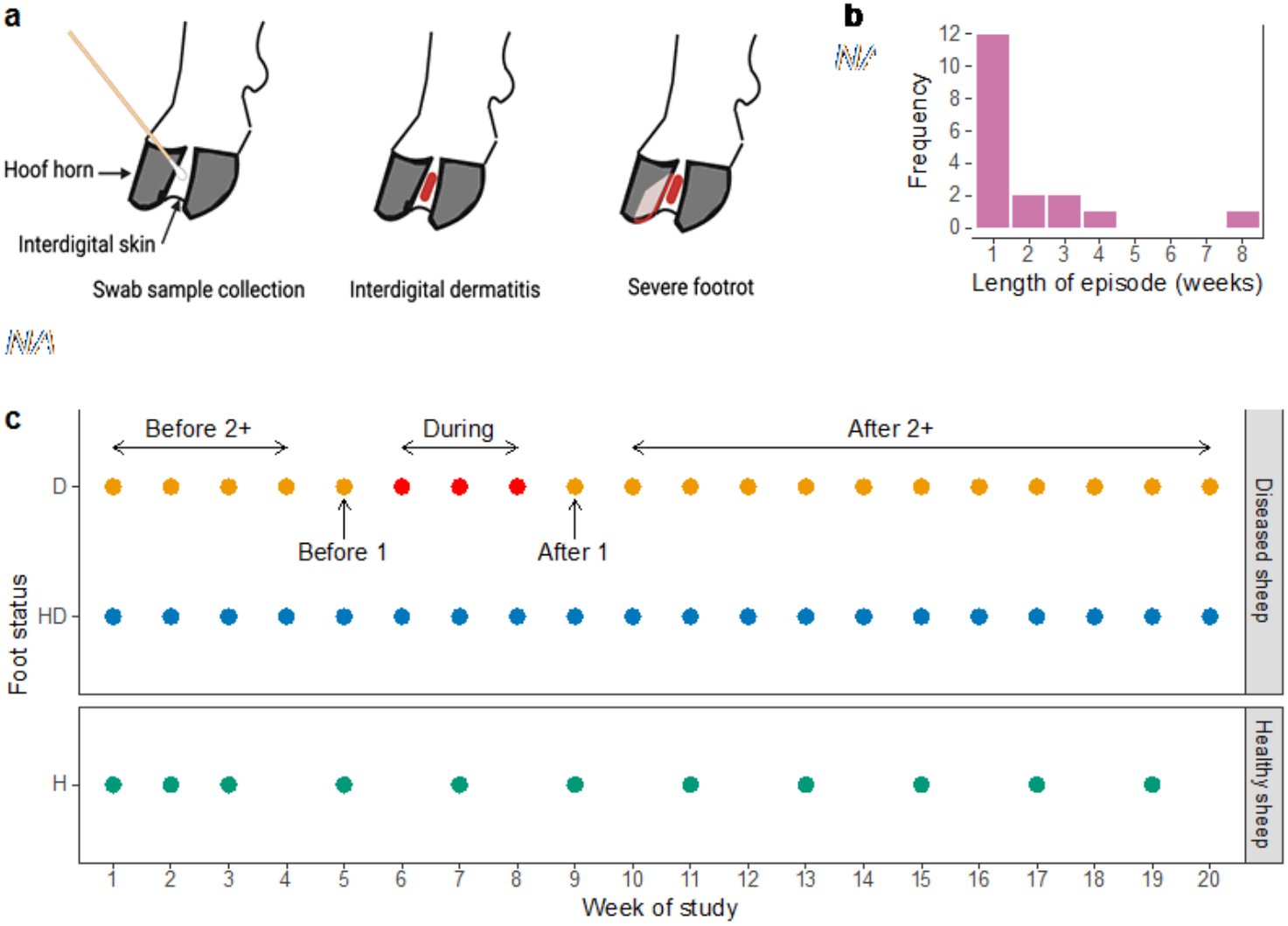

Figure 1

Classification of disease status of sheep and feet. a, Illustration of location of swab sample collection, and distribution of lesions of interdigital dermatitis and severe footrot on the sheep foot. b, Distribution of length of 18 footrot episodes in the 12 feet with footrot (D feet). c, Schematic of classification of foot status. Coloured circles show time points at which samples were analysed for three classes of foot: D (orange) = diseased foot; HD (blue) = healthy foot of diseased sheep; H (green) = healthy foot of healthy sheep. An example of a footrot episode is shown in red, and temporal classification of samples from the D foot by time relative to this episode used in the analysis is shown by arrows above and below. Before 2+ = ≥ 2 weeks before footrot episode; before 1 = 1 week before footrot episode; during = during any footrot episode; after 1 = 1 week after footrot episode, after 2+ = ≥ 2 weeks after footrot episode. Grey shaded area indicates samples included in machine learning analysis for prediction of future disease status.

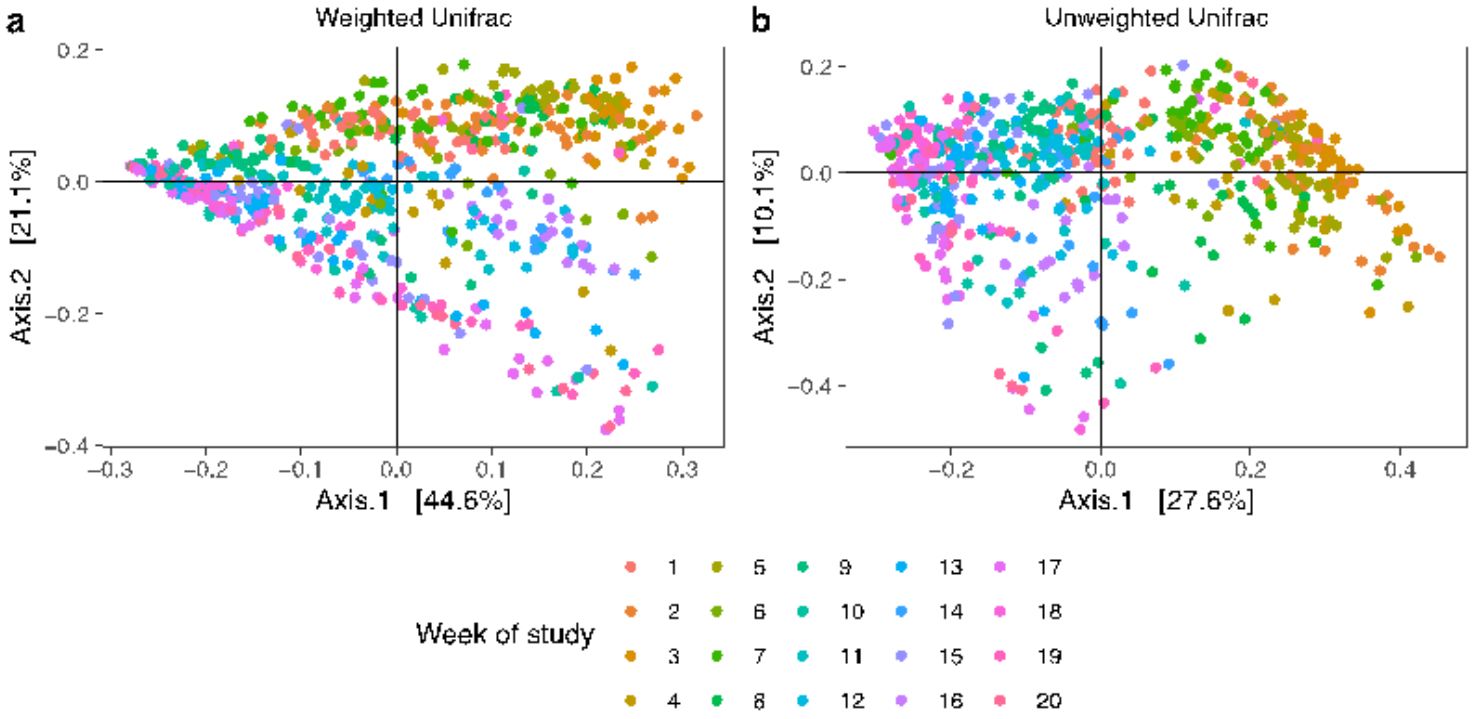

Figure 2

Temporal changes in interdigital skin microbial community composition. Principal coordinate analysis (PCoA) plot of (a) weighted and (b) unweighted Unifrac dissimilarities between microbial communities at the operational taxonomic unit (OTU) level. Each dot represents a sample coloured by week of study. Number of samples (n) = 603.

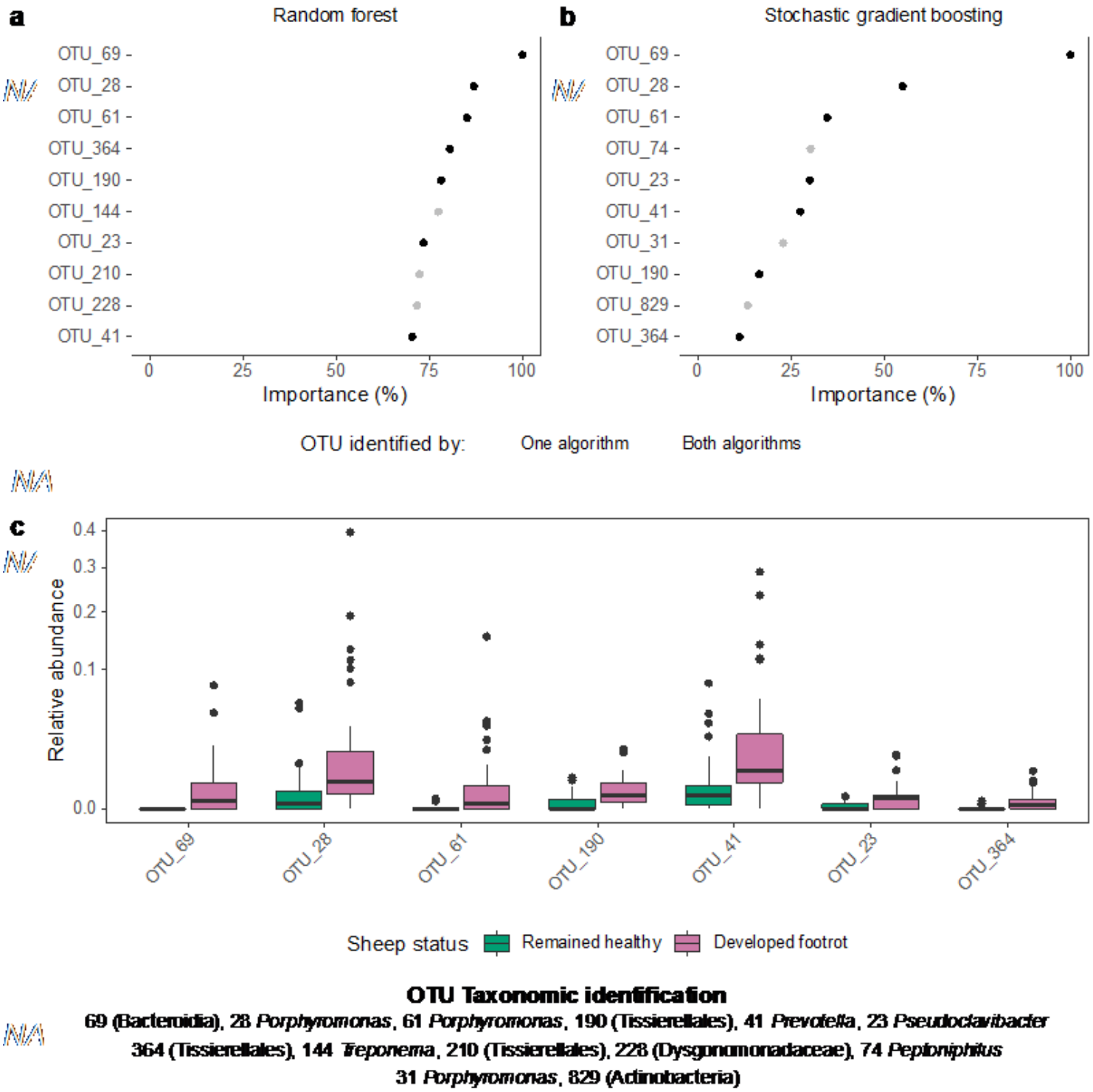

Figure 3

Composition of the IDS microbiota is predictive of footrot status of sheep. Importance of features retained in a, random forest and b, stochastic gradient boosting model for predicting disease status. Importance is scaled as a percentage relative to the importance of the most important feature. c, Boxplots of relative abundance by sheep status for operational taxonomic units (OTUs) identified by both random forest and stochastic gradient boosting model. Number of samples (n) = 117.

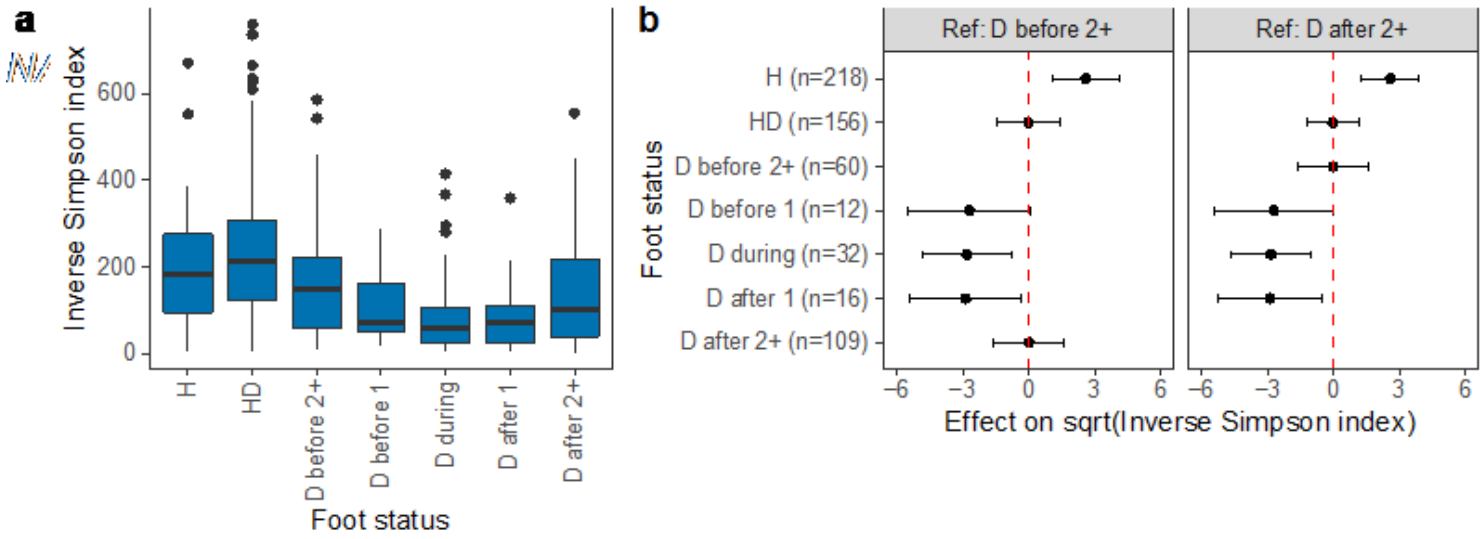

Figure 4

Diversity of the interdigital skin microbiota is temporally associated with footrot. a, Boxplots of Inverse Simpson index in samples from all sheep by foot status. b, Effects of foot status on square root transformed Inverse Simpson index as quantified by linear mixed-effects models. Centres indicate estimated fixed effects with error bars showing 95% confidence intervals. The foot status category used as the reference category in each model is shown above each plot. H = healthy foot of healthy sheep; HD = healthy foot of diseased sheep; D = diseased foot: before 2+ = ≥ 2 weeks before footrot episode; before 1 = 1 week before footrot episode; during = during any footrot episode in that foot; after 1 = 1 week after footrot episode, after 2+ = ≥ 2 weeks after footrot episode. Number of samples (n) = 603.

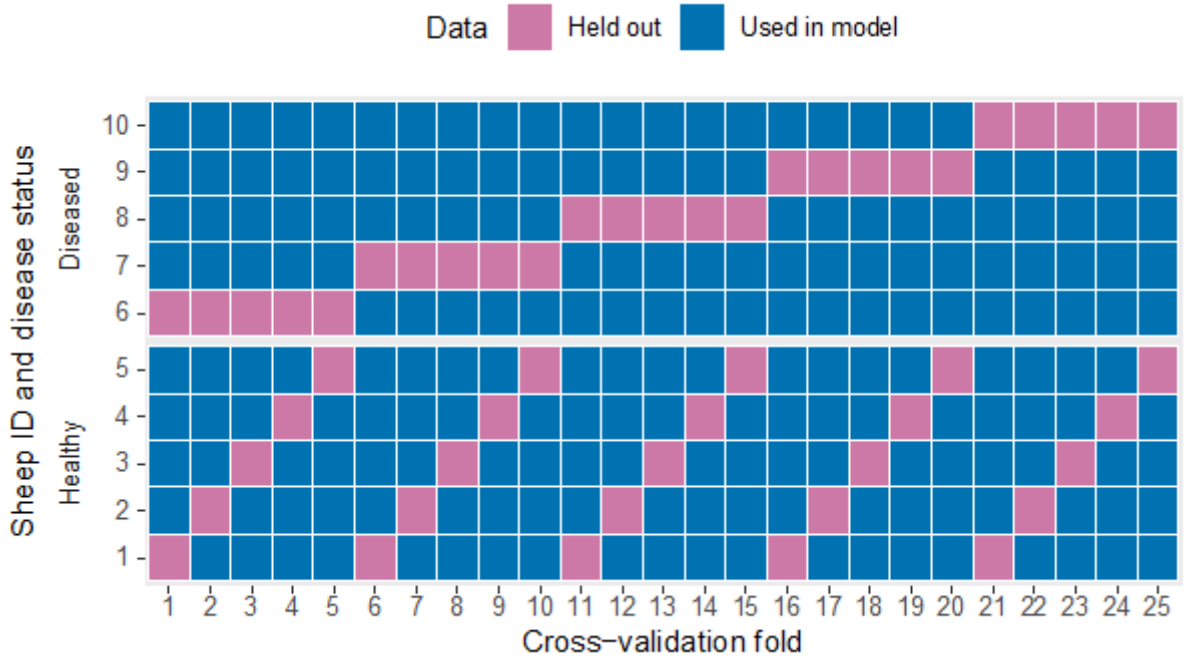

Figure 5

Schematic of cross-validation for machine learning models. The figure illustrates how data from each sheep were partitioned into modelling and holdout sets based on leaving out each of the 25 possible combinations of one healthy and one diseased sheep. This process was repeated 10 times.

Supplementary Files

This is a list of supplementary files associated with this preprint. Click to download.

- suppinfo.pdf